

A DNA-Based Two-Component Excitonic Switch Utilizing High-Performance Diarylethenes

Simon M. Büllmann, Theresa Kolmar, Nicolas F. Zorn, Jana Zaumseil, and Andres Jäschke*

Abstract: Nucleosidic diarylethenes (DAEs) are an emerging class of photochromes but have rarely been used in materials science. Here, we have developed doubly methylated DAEs derived from 2'-deoxyuridine with high thermal stability and fatigue resistance. These new photoswitches not only outperform their predecessors but also rival classical non-nucleosidic DAEs. To demonstrate the utility of these new DAEs, we have designed an all-optical excitonic switch consisting of two oligonucleotides: one strand containing a fluorogenic double-methylated 2'-deoxyuridine as a fluorescence donor and the other a tricyclic cytidine (tC) as acceptor, which together form a highly efficient conditional Förster-Resonance-Energy-Transfer (FRET) pair. The system was operated in liquid and solid phases and showed both strong distance- and orientation-dependent photochromic FRET. The superior ON/OFF contrast was maintained over up to 100 switching cycles, with no detectable fatigue.

Introduction

Photochromism is the reversible interconversion of two (meta-)stable isomers upon interaction with light. Photochromic compounds have enabled innovative applications in many different research areas^[1–2] because light as an external trigger offers unique advantages:^[3] 1) Light is non-invasive, 2) it is harmless when used appropriately, and 3) it often provides a much higher spatiotemporal resolution than e.g. chemical or electrical stimuli.^[4,5] A particularly interesting class of photochromes are diarylethenes (DAEs). In recent years, they have been researched intensely, enabling a fine

adjustment of their properties.^[6] The most common structure of classical DAEs is shown in Figure 1a, with two substituted thiophene rings connected via a cyclopentenyl bridge and two alkyl groups at the reactive α -carbon atoms. Most of today's DAEs can be classified as p-type positive photochromes that undergo a reversible cyclization reaction upon irradiation with ultraviolet (UV) or visible (Vis) light. During the cyclization process, their conjugated π -system changes, causing a strong coloration of the closed form. Many DAEs exhibit strong photochromism with high cyclization quantum yields, high thermal stability of the closed isomer, and high fatigue resistance. Originally, DAEs were intended as optical storage media^[7,8] but due to their promising photophysical properties, the application interest quickly expanded to fields such as photopharmacology,^[9,10] molecular sensors,^[11,12] high-resolution microscopy,^[13–18] and functional organic electronics.^[19,20]

In 2013 our lab introduced a new class of DAEs in which one of the aryl moieties was replaced by a pyrimidine nucleobase of a nucleoside (Figure 1b) or oligonucleotide.^[21] An inherent advantage of these molecules was that the nucleobase is an active component of the DAE core structure, allowing zero-length integration into the target (i.e., DNA). These DAEs deviated significantly from the

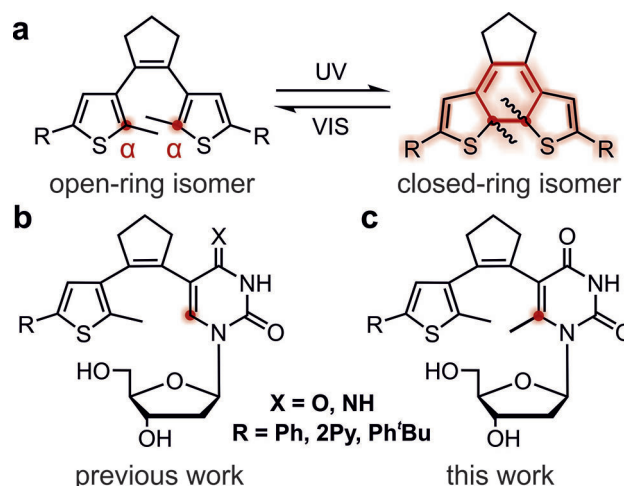


Figure 1. General overview of classical and nucleoside DAE photo-switches. a) Structural design of classical DAEs and their reversible photo-induced isomerization reaction. The reactive α -carbon atoms are highlighted. b) Previously described pyrimidine nucleoside DAEs. The unsubstituted position 6 of the nucleobase is labelled. c) Novel deoxyuridine-based photoswitches. The methylated position 6 of the nucleobase is highlighted.

[*] S. M. Büllmann, T. Kolmar, A. Jäschke
 Institute of Pharmacy and Molecular Biotechnology, Heidelberg University
 Im Neuenheimer Feld 364, 69120 Heidelberg (Germany)
 E-mail: jaeschke@uni-hd.de

N. F. Zorn, J. Zaumseil
 Institute for Physical Chemistry, Heidelberg University
 Im Neuenheimer Feld 253, 69120 Heidelberg (Germany)

© 2022 The Authors. Angewandte Chemie International Edition published by Wiley-VCH GmbH. This is an open access article under the terms of the Creative Commons Attribution Non-Commercial License, which permits use, distribution and reproduction in any medium, provided the original work is properly cited and is not used for commercial purposes.

classical DAE structural concept: one of the five-membered thiophene rings was replaced by a six-membered pyrimidine ring, and only one instead of two methyl groups were present at the reactive α -carbon atoms (Figure 1b). In a recent study, we systematically varied the substituent on the thiophene moiety of these pyrimidine-based DAEs and identified two high-performance photoswitches^[22] (dU-Ph'Bu and dU-2Py). In these photochromes, the nucleobase was left unchanged to keep them as natural as possible. However, our work on photoswitchable 2'-deoxy-7-deaza-adenosine derivatives had revealed that modifications to the nucleobase, namely the addition of a methyl group at the reactive α -carbon atom and the replacement of N-7, do not affect the natural ability of the nucleobase to form base pairs.^[23] Moreover, we observed that two methyl groups are essential for strong photochromism of purine nucleoside-based DAEs.^[24,25] These results suggested that the performance of 2'-deoxyuridine DAEs should also be improved by adding a methyl group at the α -carbon of the nucleobase in combination with a favorable substituent at the thiophene moiety (Figure 1c). Since mono-methylated deoxyuridines already outperform most classical DAEs in terms of reaction quantum yields and are on par with them in the composition of the photostationary states (PSS),^[6,7] we now aim to catch up in areas where they have been inferior, namely thermal stability and fatigue resistance. With the new generation of photoswitches, we intend to close this performance gap and thus increase their applicability in organic electronics, a discipline with the highest demands on the properties of the photochromic unit (often thousands of switching cycles and high heat tolerance).^[20,26,27] As Moore's law approaches its limit, alternative strategies for designing logic gates and integrated circuits are becoming increasingly attractive.^[28] Alternatives include all-optical excitonic switches that use photochromic Förster resonance energy transfer (pcFRET), a process in which the behavior of fluorophores is reversibly modulated by light.^[29,31] A study by Kellis et al.^[32] has shown that the construction of such a system with two fluorophores and up to three nucleosidic DAEs that act as photochromic modulators is feasible on a DNA scaffold. The use of DNA as a scaffold offers several advantages since DNA is programmable and easy to synthesize by solid-phase synthesis. Furthermore, the components can be assembled in a well-defined environment with sub-nanometer precision,^[33,34] the latter being necessary to facilitate efficient dipole-dipole coupling between neighboring chromophores. However, the reported design^[32] had some inherent limitations that restricted its overall efficiency: 1) a singly methylated nucleosidic DAE with suboptimal properties was used as a modulator, 2) the fluorophores were connected to the DNA scaffold via flexible linkers, thus losing control over the orientation factor of the pcFRET process, 3) the whole system was rather complex with its 5 components and 4) its ON/OFF contrast was satisfactory only when three modulators were present simultaneously. In this study, we present a new and robust design that greatly simplifies the construction, allows near-quantitative back-and-forth switching in both liquid and solid phases and generates a 4–12-fold increased ON/OFF contrast.

Results and Discussion

In a recent structure-function study on singly methylated 2'-deoxyuridine and -cytidine-based DAEs, we systematically varied the substituent at position 5 of the thiophene moiety and observed correlations between the electronic character of the substituent and the photophysical properties of the photochrome.^[22] Based on these findings, we decided to synthesize three doubly methylated 2'-deoxyuridine switches (dU-Me-R) with R = phenyl (Ph), 2-pyridyl (2Py), and p-benzoic acid *tert*-butylester (Ph'Bu) as substituents at the thiophene moiety and compared them with the corresponding singly methylated counterparts (dU-R). This selection should be sufficient to understand the influence of an additional methyl group on the photophysical properties of such DAEs and likely deliver high-performance photochromic candidates.

Synthesis

The mono-methylated 2'-deoxyuridine photoswitches and the boronic acid pinacolate esters (**8^R**) were prepared as described previously.^[22] The synthesis of the double-methylated photoswitches is shown in Figure 2a and started with the halogenation of commercially available 6-methyluracil (**1**). Compound (**2**) was then glycosylated with Hoffer's chloro-sugar in a silyl-Hilbert–Johnson reaction. Deprotection of (**3**) under basic conditions afforded the free nucleoside (**4**) which was subsequently coupled with boronic acid pinacolate esters (**8^R**) in a Suzuki reaction, yielding the final photoswitches. For synthetic details and standard analytical characterization see Supporting Information.

Photochromism

UV/Vis spectroscopy revealed the appearance of a new absorption maximum in the visible wavelength range between 461 nm for dU-Ph and 482 nm for dU-Me-2Py upon UV irradiation (Figure 2b, c). In direct comparison with singly methylated switches bearing the same R, the doubly methylated 2'-deoxyuridines showed a bathochromic shift of their newly generated absorption maxima of 11 nm (Ph) to 17 nm (2Py) (Figure 2b–d). Prolonged irradiation with UV-light led to the formation of a PSS^{UV} whose composition was determined by HPLC and showed the expected trend: Ph < 2Py < Ph'Bu (Figure 2d, Figure S1). The addition of a second methyl group significantly increased the switching yield and led to almost full conversion for dU-Me-Ph'Bu (97%). The information about the composition of the PSS^{UV} allowed the calculation of the spectrum of the pure closed form (red lines in Figure 2b, c). For the doubly methylated derivatives, we observed a generally higher extinction coefficient (ϵ) at the absorption maximum of the closed form. In the absence of side reactions, the composition of the PSS^{UV} is determined by two main factors: 1) the spectral separation (ratio of extinction coefficients open form/closed form) and 2) the

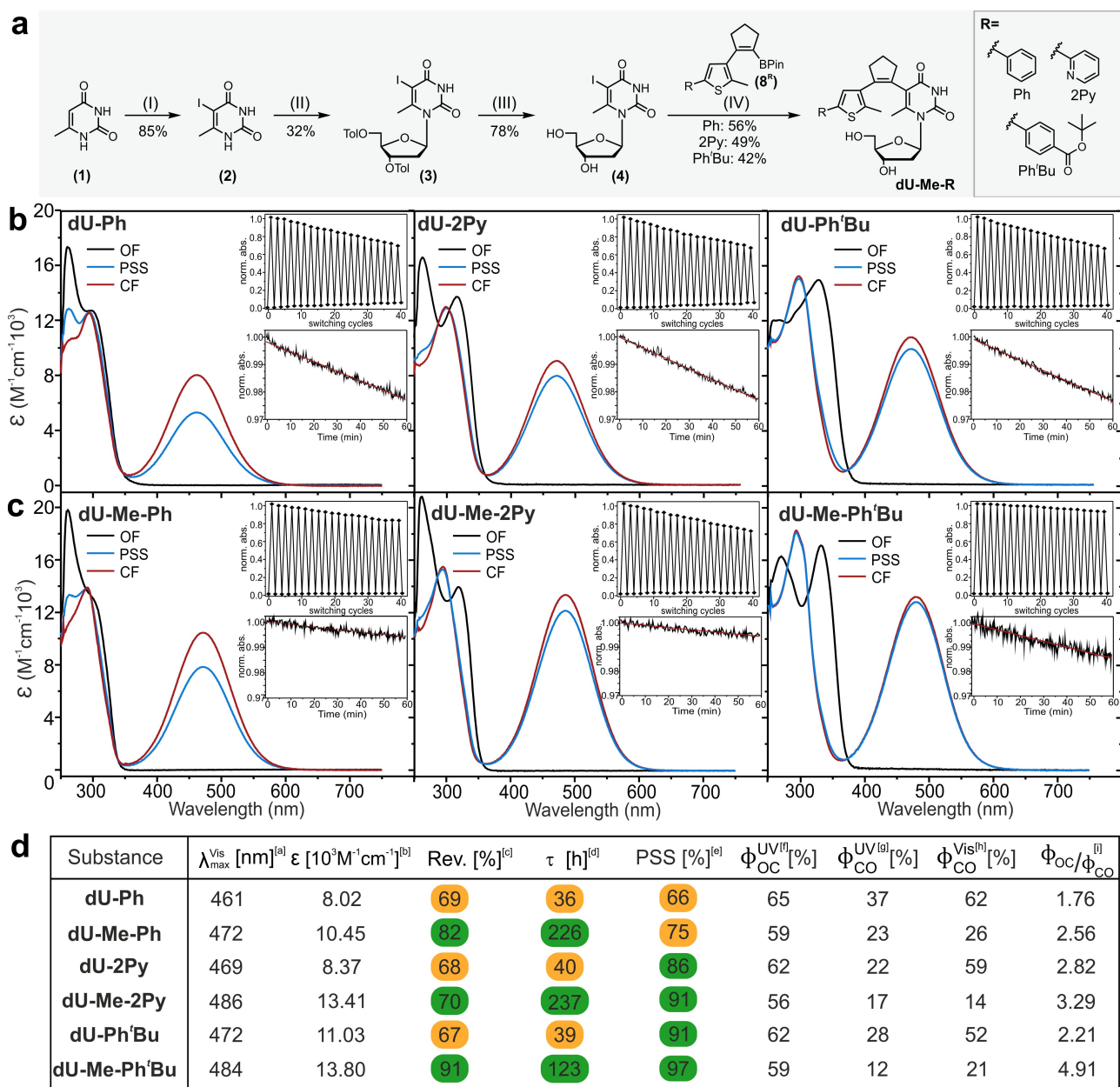


Figure 2. Synthesis of doubly methylated 2'-deoxyuridine photoswitches and overview of their photochromic properties in comparison with the singly methylated derivatives. a) Synthesis of doubly methylated 2'-deoxyuridine photoswitches. I) Cerium(IV) ammonium nitrate, iodine, MeCN, 90 °C; II) 1. hexamethyldisilazane, trimethylsilyl chloride, 120 °C; 2. Hoffer's chlorosugar, DCM, rt; III) NH₃ (aq.), MeOH, 60 °C, 150 W, microwave; IV) boronic acid pinacol ester (**8^R**), Cs₂CO₃, Pd(dppf)Cl₂, DMSO/H₂O, 100 °C. Overview of the photochromic properties of b) singly methylated 2'-deoxyuridine DAEs and c) doubly methylated 2'-deoxyuridine DAEs. Shown are absorption spectra, reversibility, and thermal stability measurements. The absorption spectra of the open form (OF, black line), PSS^{UV} after irradiation with UV light (blue line), and the calculated closed form (CF, red line) are shown. Insets show the reversibility measurement over 40 cycles at room temperature with a high-intensity light source (xenon lamp, output power at 320 nm: 10.9 mW cm⁻², output power at 530 nm: 20.5 mW cm⁻² equipped with band pass filters transmissible at 320 nm and 530 nm respectively) and a measurement of the thermal stability at 90 °C for 1 h in DMSO. d) Tabular summary of the photophysical properties of singly and doubly methylated 2'-deoxyuridine DAEs measured in DMSO. A green display symbolizes an excellent performance, while an orange display symbolizes an average performance. [a] Wavelength of the absorption maximum in the visible range. [b] Extinction coefficient of the calculated closed isomer at the absorption maximum in the visible range. [c] % photoswitch remaining intact after 40 switching cycles. Highlighted in green if > 69%. [d] Thermal half-lives of the closed isomer at 90 °C. Highlighted in green if > 100 h. [e] PSS composition after irradiation with 300 nm for dU-Ph and dU-Me-Ph and 340 nm for the remaining compounds. Highlighted in green if > 85%. [f] Ring cyclization quantum yield at 300 nm for dU-Ph and dU-Me-Ph and at 340 nm for the remaining compounds. Highlighted in green if > 85%. [g] Ring-opening quantum yield at 300 nm for dU-Ph and dU-Me-Ph and at 340 nm for the remaining compounds. [h] Ring-opening quantum yield at 505 nm. [i] Ratio of cyclization and ring-opening quantum yields at 300 nm for dU-Ph and dU-Me-Ph and at 340 nm for the remaining compounds.

ratio of the reaction quantum yields (ring closure/ring-opening) at the excitation wavelength. As can be seen in Figure 2b, c, the addition of a methyl group did not significantly change the spectral separation in the UV area. Determination of the quantum yields^[35,36] revealed, however, that this modification decreased the cycloreversion quantum yield, while cyclization remained largely unaffected (Figure 2d, Figure S2–S5). This shift of the ratio of the reaction quantum yields in favor of cyclization explains the increased switching yields. Irradiation of the closed isomer with visible light (505 nm) resulted in complete decoloration of all photochromic compounds, indicating quantitative cycloreversion ($PSS^{Vis} \approx 0\%$ closed form, see insets in Figure 2). The quantum yields for this reaction were found to be between 0.14 and 0.26, down from 0.52 to 0.62 for the singly methylated DAEs (Figure 2d). Even these reduced cycloreversion quantum yields are still an order of magnitude larger than those of typical non-nucleosidic DAEs, which are often below 1%.^[6,7,37] An efficient back-and-forth switching is of particular interest for applications in materials science, especially in experiments with fluorophores that are sensitive towards strong UV/Vis-irradiation.

Reversibility and Fatigue Resistance

After 10 switching cycles of alternating UV and Vis irradiation under our previous standard conditions,^[22,23,37] no fatigue was evident for any of the photoswitches, regardless of whether one or two methyl groups were present (Figure S6). However, these conditions were very mild (low LED power of 2.6 mW cm^{-2} at 310 nm UV-light) compared to other studies.^[38] To investigate reversibility and fatigue resistance of the compounds under harsher conditions, the photochromic molecules were irradiated with high-intensity UV/Vis light (300 W xenon lamp, measured output power: 10.9 mW cm^{-2} at 320 nm and 20.5 mW cm^{-2} at 530 nm, see insets in Figure 2b, c, Figure S7) for 40 switching cycles in DMSO. The alkylation of the α -carbon atoms was reported to increase the fatigue resistance of classical DAEs by inhibiting the dehydrogenation of the closed isomer. In this analysis, we also observed a very significant improvement of fatigue resistance in doubly methylated DAEs. In contrast to the dehydrogenation process described by Higashiguchi et al.,^[39] which takes place via an expanded valence shell of the sulfur atom, we postulate a solvent-assisted oxidation of the closed isomer, which exclusively takes place in singly methylated photoswitches (Figure S8). The presence of an additional methyl group at the α -carbon atom effectively prevents this reaction, explaining the increased fatigue resistance of the doubly methylated photoswitches. Another type of photon-induced degradation commonly reported for classical DAEs is the formation of an annulated ring system via a 1,2-dyotropic rearrangement.^[40] However, in our studies, we did not detect the formation of such a byproduct, neither in DMSO nor in aqueous solvent systems (Figure S9). The reversibility of dU-Me-Ph'Bu is comparable to that of a classical 3,5-bis(trifluoromethyl)benzene-substi-

tuted dithienylethene that had been described as particularly fatigue-resistant (Figure S10).^[38]

Thermal Stability

While temperatures rarely exceed 37°C in biological systems, they often reach much higher values in electronic devices, making closed-form thermal stability an important property for applications in materials science. Therefore, we determined thermal half-lives for all photochromic compounds at 90°C in DMSO (Figure 2d, Figure S11). The doubly methylated DAEs showed an improvement of up to six-fold with half-lives between 123 and 226 hours.

Fluorescence

Unexpectedly, when excited with UV light at 340 nm, dU-Me-Ph'Bu showed significant fluorescence with an emission maximum of 420 nm and a fluorescence quantum yield of 1% (Figure S12). Prolonged irradiation with UV light to the PSS^{UV} resulted in an 80% decrease in fluorescence intensity, which was due to the formation of the less-fluorescent closed-ring isomer (Figure S12). DAEs that are intrinsically fluorescent in their open form while non-fluorescent in the closed form can be classified as turn-OFF fluorescent photochromes, which is a desirable property for the construction of pcFRET systems. Therefore, we considered dU-Me-Ph'Bu as a candidate for the use in a pcFRET system since it combines a switchable modulator and a fluorescent donor in a single entity. The tricyclic cytidine analog (tC) should be a suitable acceptor because it has low absorption at the donor excitation wavelength (340 nm) and strong absorption at 400 nm, which overlaps well with donor emission (Figure S7). tC was already incorporated into DNA and used as an acceptor fluorophore in an orientation-dependent FRET system.^[41] Therefore, we describe below the development of an all-optical DNA-based excitonic switch using dU-Me-Ph'Bu and tC.

Photochromic Oligonucleotides

Phosphoramidite-based solid-phase synthesis was used to incorporate the donor and acceptor dyes into DNA. For this purpose, the primary hydroxyl group of nucleoside (**4**) was protected as dimethoxytrityl ether. A subsequent Suzuki reaction with (**8^{Ph'Bu}**) afforded the protected photoswitch (**5**). Finally, the secondary hydroxyl group was reacted with 2-cyanoethyl N,N-diisopropylchlorophosphoramidite to give compound (**7**) (Figure 3a). The tC phosphoramidite was prepared according to literature.^[42] The incorporation of (**7**) into four different donor strands and of tC into three acceptor strands proceeded with high coupling efficiency (Figure S13). The donor and acceptor strands were designed to be complementary to each other and to avoid undesired hybridization (see Table S1 for sequences and characterization). Expected undesired quenching of donor

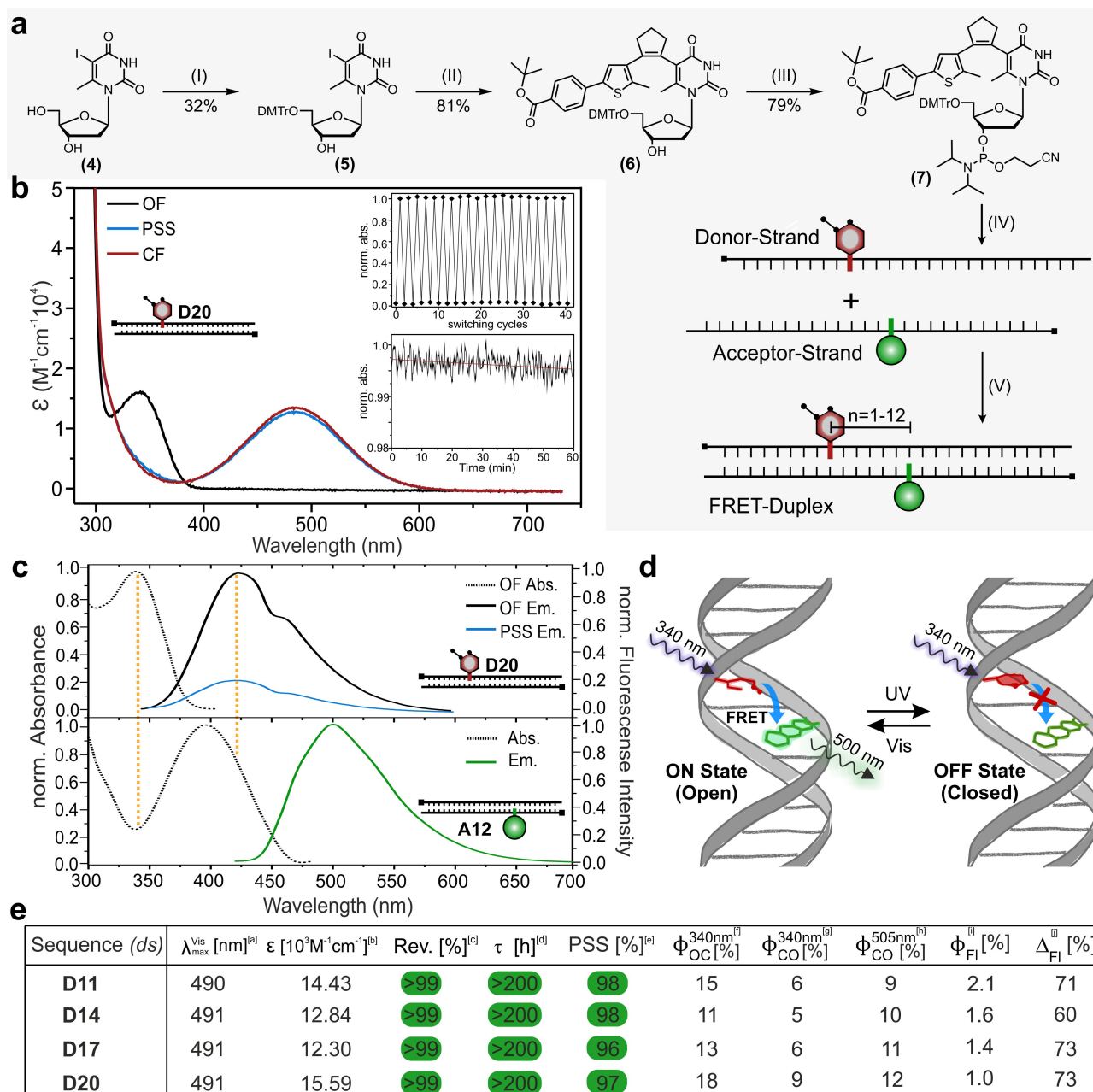


Figure 3. The overall design, preparation, and properties of an all-optical excitonic switch made of dU-Me-Ph^tBu in the donor strand and tC in the acceptor strand. a) Preparation of the FRET-capable duplex. I) dimethoxytrityl chloride, dimethylamino pyridine, pyridine, rt.; II) boronic acid pinacolate ester (**8^{Ph^tBu}**), Cs₂CO₃, Pd(dppf)Cl₂, DMSO/H₂O, 100 °C; III) 2-cyanoethyl N,N-diisopropylchlorophosphoramidite, Hünig's base, r.t., DCM; IV) solid-phase synthesis of the donor strand containing the photochromic unit (red hexagon); V) hybridization with a complementary strand containing the acceptor (green sphere). b) Overview of the photochromic properties of the donor-strand D20 in a duplex. The absorption spectra of the open form (OF, black line), PSS^{UV} (blue line) and calculated closed form (CF, red line) are shown. Insets show a reversibility measurement over 40 cycles performed at room temperature using a high-power xenon lamp (output power at 320 nm: 10.9 mW cm⁻², output power at 530 nm: 20.5 mW cm⁻², equipped with band pass filters transmissible at 320 nm and 530 nm respectively), as well as a thermal stability measurement at 90 °C for 1 h in aqueous phosphate buffer (10 mM, 0.1 M NaCl, pH 7). c) Normalized absorption and emission spectra of the donor strand (D20 upper panel) and acceptor strand (A12, lower panel) in the duplex. d) Operating mode of the all-optical excitonic switch. In the ON state (DAE open) the photochromic donor is excited at 340 nm which promotes an energy transfer via FRET to the acceptor, which then emits at 500 nm. In the OFF state (DAE closed) the energy transfer is inhibited. e) Tabular summary of the photophysical properties of all donor strands in a duplex in aqueous phosphate buffer (10 mM, 0.1 M NaCl, pH 7). A green display symbolizes an excellent performance. [a] Wavelength of the absorption maximum in the visible range. [b] Extinction coefficient of the calculated closed isomer at the absorption maximum in the visible range. [c] % photoswitch remaining intact after 40 switching cycles. Highlighted in green if > 69% [d] Thermal half-lives of the closed isomer at 50 °C. Highlighted in green if > 100 h [e] PSS composition after irradiation with 340 nm light. Highlighted in green if > 85%. [f] Ring cyclization quantum yield at 340 nm. [g] Ring-opening quantum yield at 340 nm. [h] Ring-opening quantum yield at 505 nm. [i] Fluorescence quantum yield. [j] Turn-OFF factor of the fluorescence quenching upon cyclization.

fluorescence by guanine nucleobases via an electron transfer^[43] was minimized by selecting A and T as adjacent nucleotides.^[44] Hybridization of donor and acceptor strands resulted in duplexes with different distances (number of inserted base pairs n) between the donor and acceptor fluorophore ($n=1-12$, Figure 3a, Table S2). Analysis of all possible duplexes ($n=1-12$) by CD spectroscopy confirmed the formation of DNA duplexes in the classical B-form with melting temperatures between 60.1 and 63.5 °C (Figures S14, S15, Table S3), indicating that the incorporation of dU-Me-Ph'Bu and tC did not interfere with the formation of the native duplex structure.

Photochromic Properties of the Oligonucleotides

The donor strands hybridized to an unmodified complementary strand showed pronounced photochromism (Figure 3b, e, Figure S16) with a slightly bathochromically shifted visible absorption spectrum of the closed isomers (Figure 3b, Figure S16) and reduced quantum yields of 11–18 % for cyclization and 5–9 % for cycloreversion upon UV irradiation. In contrast to oligonucleotides containing a singly methylated DAE (i.e. dU-Ph'Bu), we observed that the doubly methylated DAE retains its excellent switching yield, even in the constrained environment of a DNA duplex (96–98 % vs. 70 %, ^[22] Figure S17). This favorable behavior can be explained by a distinct spectral separation in the UV region (Figure 3b) and by a clear preference for cyclization in the quantum yields. Furthermore, all photochromic duplexes showed excellent thermal stability of their closed isomer with half-lives exceeding 200 h at 50 °C and no signs of fatigue after successively switching between the open and closed forms for 40 cycles in an aqueous solution (Figure 3b, 3e, Figure S16). The increased fatigue resistance in comparison with the nucleoside DAE is in part due to the absence of DMSO in measurements of oligonucleotides.

Fluorescence Properties of the Oligonucleotides

All donor strands showed blue fluorescence in a duplex with an unmodified complementary strand. While the fluorescence intensity of fluorescent nucleosides often decreases dramatically upon incorporation into an oligonucleotide duplex,^[43] dU-Me-Ph'Bu (Figure 3e, Figure S18, S19) and tC^[45,46] both retain their fluorescence emission as judged by the fluorescence quantum yields. Fluorescence intensity could be reversibly modulated by switching the DAE core between its two isomers, as observed at the nucleoside level (Figure S18). We observed strong quenching of fluorescence after irradiation with 340 nm UV-light, ranging from 60 % for D14 to 73 % for D20, illustrating the efficiency of these oligonucleotides as turn-OFF fluorescent photoswitches (Figure 3e).

The lower fluorescence quantum yield of donor strand D20, compared to the other donor strands, could be a consequence of the proximity of the DAE core to a guanosine two nucleotides downstream. Superposition of

the absorption and emission spectra of the donor (Figure S18) and acceptor (Figure S20) duplexes confirmed that excitation of the donor at 340 nm is required to minimize direct excitation of the acceptor. By design, in our system the donor has a local absorption maximum and the acceptor a local minimum at 340 nm (Figure 3c), thereby reducing direct excitation of the acceptor. In addition, the emission maximum of the donor overlaps well with the absorption band of the acceptor at 400 nm, allowing efficient energy transfer.

Design of an All-Optical Excitonic Switch

Our optimized design of an all-optical excitonic switch uses dU-Me-Ph'Bu as a switchable donor fluorophore and tC as an acceptor fluorophore incorporated into two complementary DNA oligonucleotides (Figure 3d). Due to the formation of a DNA duplex, both chromophores are in well-defined proximity to each other. Depending on the chemical nature of the nucleoside DAE, the system can exist in an ON state (DAE open) and an OFF state (DAE closed). The ON state is characterized by the emission of the acceptor at 500 nm as a result of an energy transfer event from the fluorescent donor. In the OFF state, on the other hand, the donor is in its less-fluorescent closed form, which means that FRET can only occur with diminished efficiency, and the emission from the acceptor is reduced. Additionally, the absorption maximum of the closed-ring isomer at 491 nm could quench the fluorescence of the acceptor. The cyclization and cycloreversion promoted by UV and Vis light lead to interconversion between the ON and OFF states. Compared to the previously described FRET-based excitonic device,^[32] our approach exploits the fluorogenic behavior of dU-Me-Ph'Bu, thus eliminating the need for an additional donor fluorophore or fluorescence modulator. This greatly simplifies the entire system by combining donor and modulator properties into a single entity. In addition, the chromophores used in the old design were linked to the ssDNA via flexible tethers, limiting control over the relative dipole orientations of the optical elements. In contrast, the chromophores used here are fixed in the DNA double helix structure via hydrogen bonds, allowing the observation of orientation-dependent energy transfer. The fluorescence spectra of duplexes $n=1-3$ (Figure 4a) show strong acceptor emission at 500 nm after excitation with 340 nm, indicating efficient energy transfer from donor to acceptor. After prolonged irradiation with UV light, the system was switched to the OFF state, and acceptor emission decreased by 45 % for $n=1$, 49 % for $n=2$, and 56 % for $n=3$ (Figure 4b). These exceptionally high ON/OFF contrasts are more than one order of magnitude higher than in the literature-known system^[32] with one photochromic modulator (four times higher than the system with 3 modulators), which illustrates the strength of the new design.

The FRET efficiencies of all possible duplexes $n=1-12$ were determined by measuring donor fluorescence in the presence of 1.15 equivalents of the acceptor strand to avoid remainders of a single-stranded donor (Figure S21). The

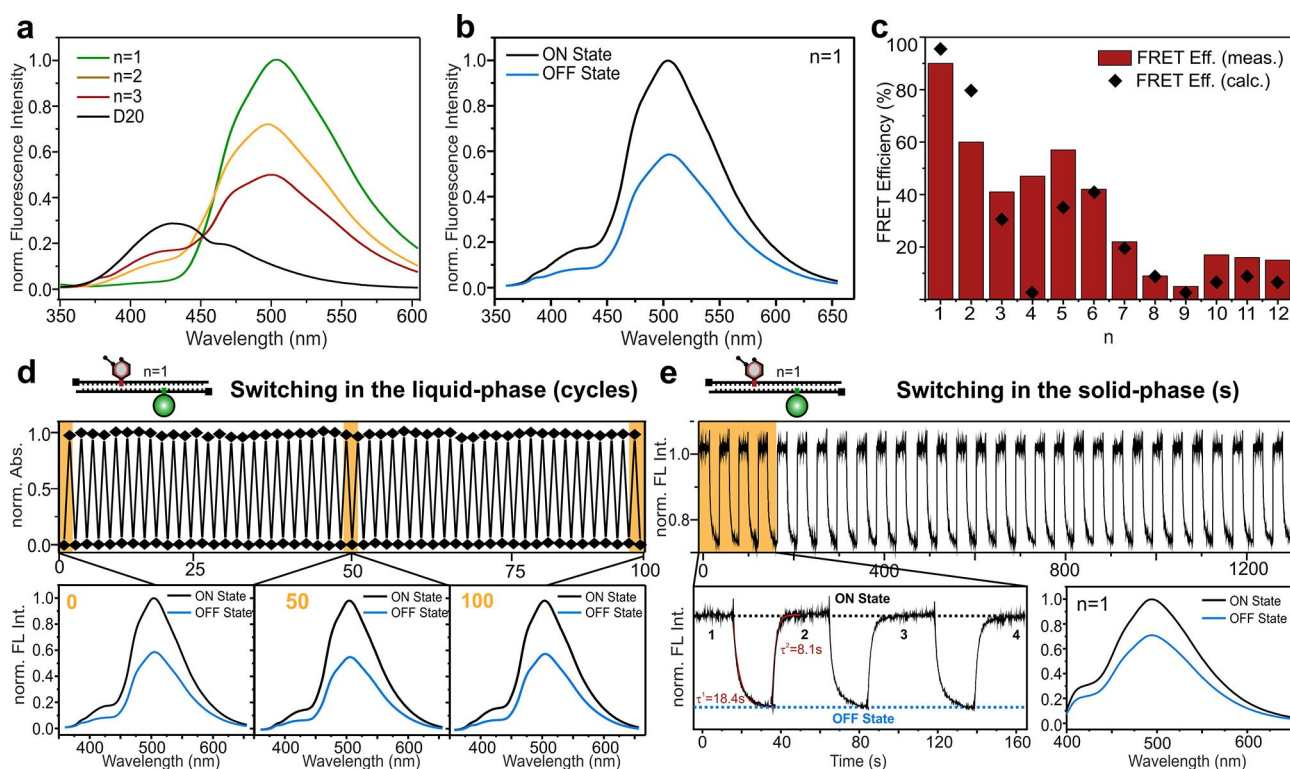


Figure 4. Performance of the FRET-based all-optical excitonic switch and cyclic fatigue assessment. a) Normalized fluorescence spectra of the duplex donor strand (black line) and FRET pairs with one (green line), two (yellow line), and three (red line) base pairs distance between donor and acceptor moieties (excitation wavelength 340 nm). b) Normalized ON- and OFF-state fluorescence of $n=1$. c) Dependence of the FRET efficiency on n (number of base pairs separating the donor and acceptor moieties). Calculated (black diamond) and measured (red bars) FRET efficiencies are shown. d) Cyclic fatigue assessment of the FRET-based all-optical excitonic switch with $n=1$ over 100 switching cycles in the liquid phase using a high-power xenon lamp (output power at 320 nm: 10.9 mW cm^{-2} , output power at 530 nm: 20.5 mW cm^{-2}). The absorption at 500 nm was normalized and plotted. Fluorescence spectra of ON- and OFF-states at 0, 50, 100 cycles are shown. e) Cyclic fatigue assessment of the FRET-based all-optical excitonic switch with $n=1$ in the solid phase over 30 cycles. The photochromic moiety was switched by exposure to 340 nm- (ON to OFF) and 470 nm- (OFF to ON) light, while recording the fluorescence intensity at 500 nm. A zoom-in of the ON and OFF state fluorescence with calculated cycling times and fluorescence spectra (excitation wavelength 340 nm) are shown.

determined FRET efficiencies show a pronounced distance and orientation dependence (Figure 4c, Table S3). If there were no orientation dependence, FRET efficiencies should decrease monotonically with increasing n . However, in our design, the FRET efficiency shows three local maxima, located at $n=1$, $n=5$, and $n=10$. At these orientations, the transition dipole moments of donor and acceptor chromophores are parallel to each other, resulting in efficient energy transfer.

This can be explained by a helical angular twist of 34.3° per base pair that occurs in right-handed B-DNA. In contrast, at $n=3$, and $n=9$ the transition dipole moments are perpendicular to each other, resulting in low FRET efficiency.^[47] This periodic change in FRET efficiency demonstrates the orientation dependence of this system. Furthermore, we calculated theoretical values of the FRET efficiency, based on a cylindrical model of the DNA double helix (Figure 4c, black diamonds). The measured FRET efficiency decreased strongly from 90% to 41% within the first three nucleotides, which is also reflected in the theoretical values and can be explained by the relatively small fluorescence quantum yield of donor strand D20.

Overall, the calculated and measured FRET efficiencies show a similar trend except for $n=4-5$. There, a relatively large difference was observed, which may be caused by a non-parallel geometry of the donor in the DNA duplex at this position or by thermal fluctuations. Similar discrepancies have also been described in the literature for other orientation-dependent FRET pairs.^[41,48] Since the configuration with one base pair between donor and acceptor chromophores showed the best performance with a FRET efficiency of 90% and an ON/OFF contrast of 45%, it was chosen to test whether this system can withstand extended cycling. The entire excitonic device was cycled between its ON and OFF states for 100 cycles without showing signs of fatigue (Figure 4d).

Existing FRET-based excitonic devices capable of information processing (in the form of a logic gate) use donor and acceptor fluorophores self-assembled on static or dynamic DNA scaffolds.^[49] Switching such devices from the ON- to the OFF-state and vice versa requires DNA dissociation, strand invasion, and displacement, slow processes that only take place in the liquid phase. A switching process that uses light, as described here, is preferable

because it does not rely on aqueous environments and enables the construction of faster-switching organic electronic devices in the solid phase. Therefore, thin films of the double-stranded DNA were prepared by drop-casting at low temperatures to ensure the integrity of the DNA duplex structure. First, absorption spectra of donor D20 in a duplex with an unmodified complementary strand were recorded. Alternating irradiation of the duplex in the solid phase efficiently converted the DAE between its isomers (Figure S22). To demonstrate its technological relevance, the all-optical excitonic switch with $n=1$ was prepared and successfully operated in the solid phase. It showed a slightly reduced ON/OFF contrast (30 % quenching) over 30 cycles and no signs of fatigue (Figure 4e, Figure S22). The dynamic modulation of the FRET-based excitonic device between its two states exhibited an exponential behavior, which was used to determine mean cycling times (τ^1 and τ^2 in Figure 4e). The mean time to switch the device to its OFF state by exposure to UV-light (340 nm) was 18.4 s, while only 8.1 s were required to recover the ON state by irradiation with Vis light (470 nm).

Conclusion

The addition of a second methyl group to 2'-deoxyuridine-based photoswitches has created a new class of powerful nucleosidic DAEs that not only outperform their singly methylated predecessors but also challenge structurally optimized classical dithienylethenes. Their exceptional properties include high fatigue resistance and thermal stability, as well as complete conversion with high quantum yields in both directions. In the constrained environment of a DNA double-strand, the new photoswitches were able to retain their performance. This tremendous increase in performance now enables applications in materials science. As a proof of principle, we have constructed a new all-optical excitonic switch that 1) operates in both the liquid and solid phases, 2) shows no cyclic fatigue, 3) consists only of two oligonucleotides each with a single chromophore, 4) exhibits a much greater ON/OFF contrast than existing constructs, and 5) provides complete control over the transition dipole moments of the FRET partners. The high chromophore density and modularity of this construct may facilitate its translation into a DNA brick nanobreadboard design for the construction of logic gates that utilize excitonic circuitry.

Acknowledgements

The authors thank H. Rudy and T. Timmermann for technical assistance and F. Billau for her help in designing the main text figures (all Heidelberg University). We also acknowledge T. Deprie (Heidelberg University) for his assistance in the early stage of the experiments. Open Access funding enabled and organized by Projekt DEAL.

Conflict of Interest

The authors declare no conflict of interest.

Data Availability Statement

The data that support the findings of this study are available in the Supporting Information of this article.

Keywords: Diarylethenes · Excitonic Switch · Nucleic Acids · Photochromic Förster Resonance Energy Transfer (PcFRET) · Photochromism

- [1] D. Trauner, *Beilstein J. Org. Chem.* **2012**, *8*, 870–871.
- [2] Y. Yokoyama in *Photon-Working Switches* (Eds.: Y. Yokoyama, K. Nakatani), Springer Japan, Tokyo, **2017**, p. 95.
- [3] C. Brieke, F. Rohrbach, A. Gottschalk, G. Mayer, A. Heckel, *Angew. Chem. Int. Ed.* **2012**, *51*, 8446–8476; *Angew. Chem.* **2012**, *124*, 8572–8604.
- [4] V. I. Minkin in *Molecular Switches* (Eds.: B. L. Feringa, W. R. Browne), Wiley-VCH, Weinheim, **2011**, pp. 37–74.
- [5] S. Loudwig, H. Bayley in *Dynamic Studies in Biology: Phototriggers, Photoswitches and Caged Biomolecules* (Eds.: M. Goeldner, R. Givens), Wiley-VCH, Weinheim, **2005**, pp. 253–340.
- [6] M. Irie, *Chem. Rev.* **2000**, *100*, 1685–1716.
- [7] M. Irie, T. Fukaminato, K. Matsuda, S. Kobatake, *Chem. Rev.* **2014**, *114*, 12174–12277.
- [8] M. Irie, M. Mohri, *J. Org. Chem.* **1988**, *53*, 803–808.
- [9] X. Chen, S. Wehle, N. Kuzmanovic, B. Merget, U. Holzgrabe, B. König, C. A. Sottriffer, M. Decker, *ACS Chem. Neurosci.* **2014**, *5*, 377–389.
- [10] Z.-Y. Li, Y.-Y. Liu, Y.-J. Li, W. Wang, Y. Song, J. Zhang, H. Tian, *Angew. Chem. Int. Ed.* **2021**, *60*, 5157–5161; *Angew. Chem.* **2021**, *133*, 5217–5221.
- [11] Z. Wang, S. Cui, S. Qiu, S. Pu, *RSC Adv.* **2019**, *9*, 6021–6026.
- [12] Z. Li, G. Davidson-Rozenfeld, M. Vázquez-González, M. Fadeev, J. Zhang, H. Tian, I. Willner, *J. Am. Chem. Soc.* **2018**, *140*, 17691–17701.
- [13] B. Roubinet, M. Weber, H. Shojaei, M. Bates, M. L. Bossi, V. N. Belov, M. Irie, S. W. Hell, *J. Am. Chem. Soc.* **2017**, *139*, 6611–6620.
- [14] K. Uno, A. Aktalay, M. L. Bossi, M. Irie, V. N. Belov, S. W. Hell, *Proc. Natl. Acad. Sci. USA* **2021**, *118*, e2100165118.
- [15] C. Li, K. Xiong, Y. Chen, C. Fan, Y.-L. Wang, H. Ye, M.-Q. Zhu, *ACS Appl. Mater. Interfaces* **2020**, *12*, 27651–27662.
- [16] H. Yang, M. Li, C. Li, Q. Luo, M.-Q. Zhu, H. Tian, W.-H. Zhu, *Angew. Chem. Int. Ed.* **2020**, *59*, 8560–8570; *Angew. Chem.* **2020**, *132*, 8638–8648.
- [17] C. Li, H. Yan, L.-X. Zhao, G.-F. Zhang, Z. Hu, Z.-L. Huang, M.-Q. Zhu, *Nat. Commun.* **2014**, *5*, 5709.
- [18] C. Li, W.-L. Gong, Z. Hu, M. P. Aldred, G.-F. Zhang, T. Chen, Z.-L. Huang, M.-Q. Zhu, *RSC Adv.* **2013**, *3*, 8967–8972.
- [19] D. D. Dashitsyrenova, A. G. Lvov, L. A. Frolova, A. V. Kulikov, N. N. Dremova, V. Z. Shirinian, S. M. Aldoshin, M. M. Krayushkin, P. A. Troshin, *J. Mater. Chem. C* **2019**, *7*, 6889–6894.
- [20] W. Rekab, T. Leydecker, L. Hou, H. Chen, M. Kirkus, C. Cendra, M. Herder, S. Hecht, A. Salleo, I. McCulloch, E. Orgiu, P. Samorì, *Adv. Funct. Mater.* **2020**, *30*, 1908944.
- [21] H. Cahová, A. Jäschke, *Angew. Chem. Int. Ed.* **2013**, *52*, 3186–3190; *Angew. Chem.* **2013**, *125*, 3268–3272.

- [22] T. Kolmar, S. M. Büllmann, C. Sarter, K. Höfer, A. Jäschke, *Angew. Chem. Int. Ed.* **2021**, *60*, 8164–8173; *Angew. Chem.* **2021**, *133*, 8245–8254.
- [23] S. M. Büllmann, T. Kolmar, P. Slawetzki, S. Wald, A. Jäschke, *Chem. Commun.* **2021**, *57*, 6596–6599.
- [24] M. Singer, A. Jäschke, *J. Am. Chem. Soc.* **2010**, *132*, 8372–8377.
- [25] C. Sarter, M. Heimes, A. Jäschke, *Beilstein J. Org. Chem.* **2016**, *12*, 1103–1110.
- [26] H. Qiu, Y. Zhao, Z. Liu, M. Herder, S. Hecht, P. Samori, *Adv. Mater.* **2019**, *31*, 1903402.
- [27] L. Hou, X. Zhang, G. F. Cotella, G. Carnicella, M. Herder, B. M. Schmidt, M. Pätzelt, S. Hecht, F. Cacialli, P. Samori, *Nat. Nanotechnol.* **2019**, *14*, 347–353.
- [28] M. M. Waldrop, *Nature* **2016**, *530*, 144–147.
- [29] K. Szaciłowski, *Chem. Rev.* **2008**, *108*, 3481–3548.
- [30] C. Pistol, C. Dwyer, A. R. Lebeck, *IEEE Micro* **2008**, *28*, 7–18.
- [31] P. D. Cunningham, W. P. Bricker, S. A. Diaz, I. L. Medintz, M. Bathe, J. S. Melinger, *J. Chem. Phys.* **2017**, *147*, 055101.
- [32] D. L. Kellis, C. Sarter, B. L. Cannon, P. H. Davis, E. Graugnard, J. Lee, R. D. Pensack, T. Kolmar, A. Jäschke, B. Yurke, W. B. Knowlton, *ACS Nano* **2019**, *13*, 2986–2994.
- [33] J. Bath, A. J. Turberfield, *Nat. Nanotechnol.* **2007**, *2*, 275–284.
- [34] B. Wei, M. Dai, P. Yin, *Nature* **2012**, *485*, 623–626.
- [35] U. Megerle, R. Lechner, B. König, E. Riedle, *Photochem. Photobiol. Sci.* **2010**, *9*, 1400–1406.
- [36] H. Volfova, Q. Hu, E. Riedle, *EPA Newsl.* **2019**, 51–69.
- [37] S. M. Büllmann, A. Jäschke, *Chem. Commun.* **2020**, *56*, 7124–7127.
- [38] M. Herder, B. M. Schmidt, L. Grubert, M. Pätzelt, J. Schwarz, S. Hecht, *J. Am. Chem. Soc.* **2015**, *137*, 2738–2747.
- [39] K. Higashiguchi, K. Matsuda, T. Yamada, T. Kawai, M. Irie, *Chem. Lett.* **2000**, *29*, 1358–1359.
- [40] K. Higashiguchi, K. Matsuda, S. Kobatake, T. Yamada, T. Kawai, M. Irie, *Bull. Chem. Soc. Jpn.* **2000**, *73*, 2389–2394.
- [41] S. Hirashima, H. Sugiyama, S. Park, *J. Phys. Chem. B* **2020**, *124*, 8794–8800.
- [42] P. Sandin, P. Lincoln, T. Brown, L. M. Wilhelmsson, *Nat. Protoc.* **2007**, *2*, 615–623.
- [43] W. Thongyod, C. Buranachai, T. Pengpan, C. Punwong, *Phys. Chem. Chem. Phys.* **2019**, *21*, 16258–16269.
- [44] S. Hirashima, J. H. Han, H. Tsuno, Y. Tanigaki, S. Park, H. Sugiyama, *Chem. Eur. J.* **2019**, *25*, 9913–9919.
- [45] P. Sandin, L. M. Wilhelmsson, P. Lincoln, V. E. Powers, T. Brown, B. Albinsson, *Nucleic Acids Res.* **2005**, *33*, 5019–5025.
- [46] L. M. Wilhelmsson, A. Holmén, P. Lincoln, P. E. Nielsen, B. Nordén, *J. Am. Chem. Soc.* **2001**, *123*, 2434–2435.
- [47] M. Bood, S. Sarangamath, M. S. Wranne, M. Grotli, L. M. Wilhelmsson, *Beilstein J. Org. Chem.* **2018**, *14*, 114–129.
- [48] K. Börjesson, S. Preus, A. H. El-Sagheer, T. Brown, B. Albinsson, L. M. Wilhelmsson, *J. Am. Chem. Soc.* **2009**, *131*, 4288–4293.
- [49] B. L. Cannon, D. L. Kellis, P. H. Davis, J. Lee, W. Kuang, W. L. Hughes, E. Graugnard, B. Yurke, W. B. Knowlton, *ACS Photonics* **2015**, *2*, 398–404.

Manuscript received: December 28, 2021

Accepted manuscript online: January 25, 2022

Version of record online: February 10, 2022